THE EFFECTS OF PROJECTILE SPEED AND MEDIUM RESISTANCE IN RICOCHET OFF SAND

Y. L. Bai†‡   W. Johnson†§

It has been observed experimentally that when a sphere ricochets off water or sand the critical impact angle depends on the impinging velocity.
To explain this, a model is developed which takes into account the weight of the sphere and the static resistance of the medium into which penetration occurs. The proposed model can also treat processes in which the angle of impact is large and where the velocity of the sphere undergoes considerable change. Projectile trajectories which have been calculated for various conditions are presented and discussed. Numerical results for steel, aluminium alloy, and lead spheres are in good agreement with such experimental results as are available.

1 INTRODUCTION

When a spherical projectile ricochets off water, there exists a critical angle θ_c, beyond which ricochet would not occur and the projectile sink. This critical angle has been established, empirically, as

$$\theta_c \simeq 18°/\sqrt{\sigma} \tag{1}$$

where σ is the ratio of projectile and medium densities—see Johnson and Reid (1)‖ who have given a fairly comprehensive review of this subject up to 1975. It is worth noticing that, in the empirical formula (1), the critical angle is stated only to be dependent on a ratio of densities there being no explicit reference to the velocity of the projectile.

Johnson and Reid (1) re-presented Birkhoff's original theory and suggested a simple but satisfactory model to describe the above phenomenon and to predict the critical angle θ_c. The theory provides

$$\theta_c = 0.326/\sqrt{\sigma} = 17.5°/\sqrt{\sigma} \tag{2}$$

which renders it in excellent agreement with the expression (1) obtained experimentally.

However, recent experimental investigations have explored the dependence of the critical angle on velocity and have indicated that it has different tendencies in different media. For example, Soliman, Johnson, and Reid (2) found that when a spherical projectile ricochets off water, the critical impact angle θ_c decreases with decreasing impact speed. But, contrariwise when the same projectile ricochets off sand, the dependence is reversed, namely, the critical impact angle θ_c decreases with increasing impact speed. .Concluding their experimental results, the latter authors observed that they were led to believe that the forces responsible for ricochet vary significantly with impact speed and that the critical impact angle depends greatly on impact speed, spin, and the depth of immersion of the projectile in the medium. Thus the influence of all these merited further study. For a preliminary examination of the influence of these factors they included the gravitational force on the projectile in setting-up the dynamic equations of the

projectile following the Birkhoff approach and found the critical impact angle to be velocity-dependent, according to

$$\theta_g{}^2 = \theta_c{}^2 - \frac{4}{F} \tag{3}$$

where $F = \bar{v}^2/ag$ is the average Froude number, $\bar{v}$ is the average velocity of the projectile during its passage through the medium surface, a is the radius of the sphere, and g the gravitational acceleration. In this way they explained the decreasing velocity dependence of critical impact angle. However, they did not give any explanation of the increasing velocity-dependence of the critical angle for ricochet off sand.

In order to appreciate the above-mentioned phenomena and to make the description quantitative, it is useful to examine the Birkhoff approach carefully.

The latter embraces the following assumptions.

(1)   Quasi-steady flow is assumed.
(2)   Hydrodynamic pressure only is taken to be responsible for ricochet.
(3)   The latter hydrodynamic pressure is expressed as

$$p = \tfrac{1}{2}\rho v^2 \cos^2 \beta \tag{4}$$

where p denotes pressure, ρ the density of the medium, v the fluid flow velocity, and β is the angle between the projectile velocity vector and the normal to the surface of the moving projectile.
(4)   Any splash created is assumed to have no effect on ricochet performance.
(5)   The angle between the projectile velocity vector and the horizontal remains small during the course of ricochet.
(6)   The velocity of the projectile remains constant during its encounter with the medium.
(7)   When the sphere is just fully submerged in the medium the inclined angle θ of the projectile velocity vector is zero, and this corresponds to the occurrence of critical ricochet.

In this paper, it is intended to re-examine the above assumptions and to attempt to clarify the importance of the various forces which might be responsible for ricochet.

In section 2, a simple small angle case is discussed. It is hoped that this simple but clear approach will aid further exact understanding. In section 3, a more general and exact description is put forward. In section 4 the

results of some calculations are presented to facilitate a comparison between experimental and theoretical results.

1.1 Notation

a	Radius of sphere
g	Gravitational acceleration
p	Pressure
t	Time
v	Projectile velocity
x, y	Cartesian coordinates
F	$=v^2/ag$; Froude number
FN	$=4\sigma ag/(K/\rho)$
K	Static material resistance
L	Lift
M	Mass of projectile
R	Horizontal resistance
V	Dimensionless projectile velocity
β	Angle between normal to surface element and velocity of sphere
ζ, ξ	Coordinates fixed on sphere
η	Dimensionless vertical position of sphere
θ	Angle of velocity inclined to horizontal
θ_c	Critical impact angle
ρ	Density of medium
ρ'	Density of sphere
σ	Ratio of densities of sphere and medium
ϕ, ψ	Angular variable in coordinates fixed on sphere
F_ζ, F_ξ	Forces exerted on sphere
$f_{\zeta p}, f_{\xi p}$	Function of angular variable

2 ANALYSIS FOR SMALL ANGLE OF IMPACT

In this section a small impact angle case is discussed and a modification of Birkhoff's assumptions is made in that not only is hydrodynamic pressure taken into account but the gravitational weight of the projectile and the static pressure in the medium through which the projectile travels also.

Based on a quasi-steady flow assumption, Bernoulli's theorem is so adapted that the pressure at the stagnation point consists of two parts namely a hydrodynamic pressure of $\rho v^2/2$ and a static pressure, K. Thus

$$p=\tfrac{1}{2}\rho v^2+K \tag{5}$$

where v is the flow velocity and K could derive from the internal resistance of the material. (K in equations (5)
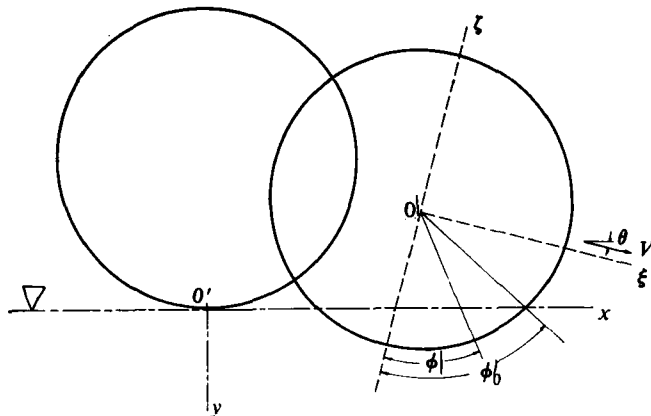

Fig. 1. Side view of a partially submerged sphere defining ϕ, ϕ_0, and θ

and (6) is similar to R_T, the target plate resistance introduced by Tate (3) for considering hypervelocity impact penetration.) Because of the quasi-steady flow, assumption (5) is suitable for a moving body at the corresponding stagnation point. On other parts of the moving body following Birkhoff et al., the pressure is expressed as

$$p=\tfrac{1}{2}\rho v^2 \cos^2 \beta+K \tag{6}$$

where the resistance or pressure K is considered to be isotropic.

The equation of motion of the projectile is,

$$M\frac{\mathrm{d}^2 y}{\mathrm{d}t^2}=-L+Mg \tag{7}$$

where M denotes the mass of the projectile, L the lift, and the coordinates are as shown in Fig. 1. The suppositions of constant velocity and small impact angle lead to

$$\frac{\mathrm{d}y}{\mathrm{d}x}=\tan\theta\simeq\theta \tag{8}$$

and

$$\frac{\mathrm{d}^2 y}{\mathrm{d}t^2}=v^2\frac{\mathrm{d}^2 y}{\mathrm{d}x^2}=v^2\frac{\mathrm{d}(\mathrm{d}y/\mathrm{d}x)^2}{2\mathrm{d}x}\frac{\mathrm{d}x}{\mathrm{d}y} \tag{9}$$

The equation of horizontal motion then becomes

$$\mathrm{d}(\theta^2)=-2\frac{L}{Mv^2}\,\mathrm{d}y+2\frac{g}{v^2}\,\mathrm{d}y \tag{10}$$

For a spherical projectile, the lift is

$$\mathrm{d}L=p\cos\phi.a^2\sin\phi.\mathrm{d}\phi\,\mathrm{d}\psi$$

$$=\left(\frac{\rho v^2}{2}\sin^2\phi\cos^2\psi+K\right).\cos\phi\sin\phi\,a^2\mathrm{d}\phi\,\mathrm{d}\psi \tag{11}$$

because $\cos\beta=\sin\phi\cos\psi$, where ϕ and ψ are the angular variables in spherical coordinates. The wetted area is assumed to be that at the surface level, namely

$$0\leqslant\phi\leqslant\phi_0 \text{ (see Fig. 1).} \tag{12}$$

Simple geometry gives

$$\cos\phi_0=-\eta=-\frac{y}{a} \tag{13}$$

and thus the final equation becomes

$$\mathrm{d}\theta^2=-\left(\frac{3}{32}\frac{(1-\eta^2)^2}{\sigma}+\frac{3K(1-\eta^2)}{4\sigma\rho v^2}-\frac{2ag}{v^2}\right)\mathrm{d}\eta. \tag{14}$$

Integrating (14) in the region $[-1, 1]$ of η, with the boundary condition of $\theta=0$ at $\eta=1$, yields the critical angle θ_c as

$$\theta_c^2=\frac{1}{10\sigma}+\frac{K}{\rho v^2\sigma}-\frac{4ag}{v^2} \tag{15}$$

The third term is the reciprocal of the Froude number and the second involves the resistance K of the medium for the circumstances considered. If

$$\frac{K}{\rho v^2\sigma}\ll 1 \tag{16}$$

then the medium behaves as if it was a fluid.

If both $K/\rho v^2\sigma$ and $4ag/v^2$ can be neglected, which implies that the medium has no static resistance and that

$\sigma = 2 \cdot 889$
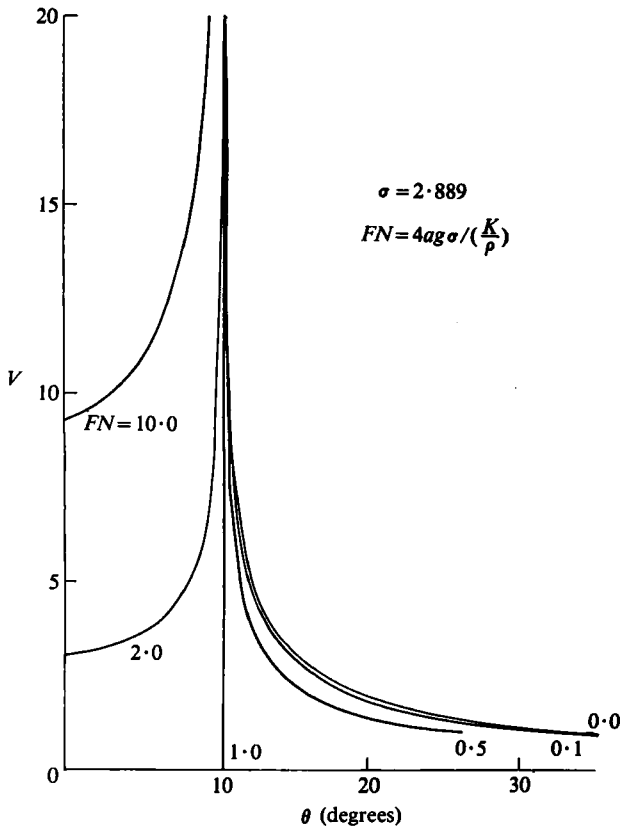
$FN = 4ag\sigma / (\frac{K}{\rho})$

Fig. 2. Curves of velocity dependence of critical impact angle due to different sphere densities and medium resistance

the weight of the projectile is unimportant, then the critical impact angle is as obtained by Birkhoff *et al.* (1). This physical circumstance can be arrived at only when very high velocities at impact prevail, but otherwise, the critical angle is velocity-dependent.

If in the case concerned the weight of the projectile is more significant than the static resistance of the medium, as in the situation of ricochet off water, then equation (15) predicts a decreasing velocity-dependence of critical impact angle (see Fig. 2). Alternatively, in the case of ricochet off sand, the static material resistance is more important than the weight of the projectile; sand can support the projectile easily whereas water cannot. Thus, the above model gives a reversed dependence. These conclusions are in agreement with the various mentioned observations. For an arbitrary ricochet case, which branch of the $\theta \sim v$ curve will be followed depends on the ratio $K/4ag\sigma\rho$, namely the ratio of the static resistance of the medium to the weight of the projectile. However, high speed impact gives upper and lower limits to the critical impact velocity in either case.

3 ANALYSIS FOR LARGE ANGLES OF IMPACT

Where the static resistance of the medium plays an important role, the critical impact angle increases with decreasing impact velocity. However, in sand the lower limit to the critical impact angle is 10·6 degrees for steel spheres and 18 degrees for aluminium spheres (2). Thus, the use of small angle theory is less justified and may lead to errors. To investigate the phenomenon more accurately, some modifications are now made to the Birkhoff assumptions (2), (5) and (6) above. Static

pressure is now taken into account and the assumptions that impact angle is small and the projectile velocity constant are abandoned.

Instead of equation (7), a system of equations is called for

$$\begin{cases} M \dfrac{d^2y}{dt^2} = -L + Mg \\ M \dfrac{d^2x}{dt^2} = -R \end{cases} \tag{17}$$

where L and R denote lift and horizontal resistance or drag, respectively. Because of the implied trajectory relations

$$\begin{cases} y = y(t) \\ x = x(t) \end{cases} \tag{18}$$

equations (17) can be transformed into

$$\begin{cases} M\, d(v \cos\theta)^2 = -2(L - Mg)\, dy \\ M\, d(v \cos\theta)^2 = -2R\, dy/\tan\theta \end{cases} \tag{19}$$

In order to calculate the lift, L, and resistance, R, a new coordinate system ξ, ζ and Z is introduced (see Fig. 1), where the Z axis is perpendicular to the x, y plane. The origin lies at the centre of the sphere whilst the ξ axis always retains the sphere velocity direction. In this way pressure can be expressed as

$$p = \frac{\rho v^2}{2} \cos^2\beta + K \tag{20}$$

with

$$\cos\beta = \cos\psi \sin\phi \tag{21}$$

where ψ and ϕ are angular variables in coordinates ξ, ζ, and Z. The forces (except for gravity) exerted on the sphere along the ζ and ξ axes are

$$dF_\zeta = p \cos\phi \cdot a^2 \sin\phi \cdot d\phi\, d\psi$$
$$= \left\{ \frac{\rho v^2}{2} \cos^2\psi \sin^3\phi \cos\phi + K \sin\phi \cos\phi \right\} a^2\, d\phi\, d\psi \tag{22}$$

and

$$dF_\xi = p \sin\phi \cos\psi\, a^2 \sin\phi\, d\phi\, d\psi$$
$$= \left\{ \frac{\rho v^2}{2} \cos^3\psi \sin^4\phi + K \cos\psi \sin^2\phi \right\} a^2\, d\phi\, d\psi \tag{23}$$

The range of integration is $(-\pi/2, \pi/2)$ for ψ, but for ϕ is more complicated. Noting that

$$\delta = arc \cos(-\eta) \tag{24}$$

and

$$\phi_0 = \theta + \delta \tag{25}$$

instead of (13) in this case ϕ_0 refers to the angle from the ζ axis to the point on the surface of the sphere at which the surface level of the medium just touches it. So, if $\phi_0 > 2\phi$

$$0 = \phi_l \leqslant \phi \leqslant \phi_0 \tag{26}$$

defines the wetted area; with $\phi_0 < 2\theta$, the wetted area is determined by

$$\phi_0 - 2\delta = \phi_l \leqslant \phi \leqslant \phi_0 \tag{27}$$

where ϕ_l is the lower limit of the wetted area. Integrating (22) and (23) and adopting the unified notation ϕ_l and ϕ_0 F_ζ and F_ξ become

$$F_\zeta = \left(\frac{\rho v^2}{2}\right) a^2 f_{\zeta\rho} + Ka^2 f_{\zeta K} \qquad (28)$$

and

$$F_\xi = \left(\frac{\rho v^2}{2}\right) a^2 f_{\xi\rho} + Ka^2 f_{\xi K} \qquad (29)$$

where

$$\left.\begin{aligned} f_{\zeta\rho} &= \frac{\pi}{8}\sin^4\phi_0 - \frac{\pi}{8}\sin^4\phi_l \\[4pt] f_{\zeta K} &= \frac{\pi\sin^2\phi}{2} - \frac{\pi\sin^2\phi_l}{2} \\[4pt] f_{\xi\rho} &= \left(\frac{3\phi}{2} - \frac{3\sin^2\phi}{4} - \sin^3\phi\cos\phi\right)\Big/3 \\[4pt] &\quad - \left(\frac{3\phi_l}{2} - \frac{3\sin 2\phi_l}{4} - \sin^3\phi_l\cos\phi_l\right)\Big/3 \end{aligned}\right.$$

and

$$f_{\xi K} = \left(\phi_0 - \frac{\sin 2\phi}{2}\right) - \left(\phi_l - \frac{\sin 2\phi_l}{2}\right)$$

$$\tag{30}$$

The lift, L, and resistance, R, are connected with F_ζ and F_ξ thus

$$\begin{aligned} L &= F_\zeta\cos\theta + F_\xi\sin\theta \\ R &= -F_\zeta\sin\theta + F_\xi\cos\theta \end{aligned} \qquad (31)$$

After substituting (28), (29) and (31) into (17), the governing equations become

$$d(V\sin\theta)^2 = -\frac{3}{2\pi\sigma}\left\{\cos\theta\left(\frac{V^2}{2}f_{\zeta\rho} + f_{\zeta K}\right)\right.$$

$$\left. + \sin\theta\left(\frac{V^2}{2}f_{\xi\rho} + f_{\xi K} - \frac{\pi}{3}FN\right)\right\}d\eta \qquad (32)$$

and

$$d(V\cos\theta)^2 = -\frac{3}{2\pi\sigma}\left\{-\sin\theta\left(\frac{V}{2}^2 f_{\zeta\rho} + f_{\zeta K}\right)\right.$$

$$\left. + \cos\theta\left(\frac{V^2}{2}f_{\xi\rho} + f_{\xi K}\right)\right\}d\eta/\tan\theta$$

where $\sigma = \rho'/\rho$, $V^2 = (\rho v^2)/K$, $FN = (4\sigma ag)/(K/\rho)$ and $f_{\xi\rho}$, $f_{\zeta K}, f_{\xi\rho}, f_{\xi K}$ are expressed in (30).

The initial conditions are at,

$$\eta = -1, \quad V = V_0 \quad \text{and} \quad \theta = \theta_0 \qquad (33)$$

The system of equations (32) require to be integrated numerically with the initial conditions specified by (33).

4 INTERPRETATION OF RESULTS

The relationship between impact velocity and the critical impact angle for ricochet for the small angle impact case is shown in Fig. 2. It is clear that the critical impact angle decreases from the angle which corresponds to $K/4ag\sigma\rho = 1$, with decreasing or increasing impact velocity according to $K/4ag\sigma\rho < 1$ or > 1. These correspond to ricochet off water and off sand in the tests described in (2), respectively. For a steel projectile off sand $K/4ag\sigma\rho = 1$ corresponds to $\theta \sim 10$ degrees (see Fig. 2).

For the case of the large impact angles discussed in section 3, the problem and the computation become complicated. For the non-linear combined equations (32), numerical integration is carried out by the Runge–Kutta method. In performing the calculations, the weight of the projectile is ignored. In this situation it is unsatisfactory to integrate the equations (32) from $\eta = 1$, $\theta = 0$ in order to obtain the critical impact angle of ricochet. The reason for this is that in the Birkhoff approach it was assumed that $\eta = 1$ and $\theta = 0$ is the criterion of ricochet, no matter what the velocity is. But in the large impact velocity case, this is no longer so. The projectile could stop inside the material, even when $\eta = 1$ and $\theta = 0$ or $\eta < 1$ and, therefore, the Birkhoff assumption (7) must be modified.

For the afore-mentioned reasons, some form of computational experiments with initial condition (33) are needed in order to observe behaviour at the end of the trajectory.

During the course of movement, the projectile velocity decreases gradually for any impact angle and velocity. However, trajectories can be grouped under several headings.
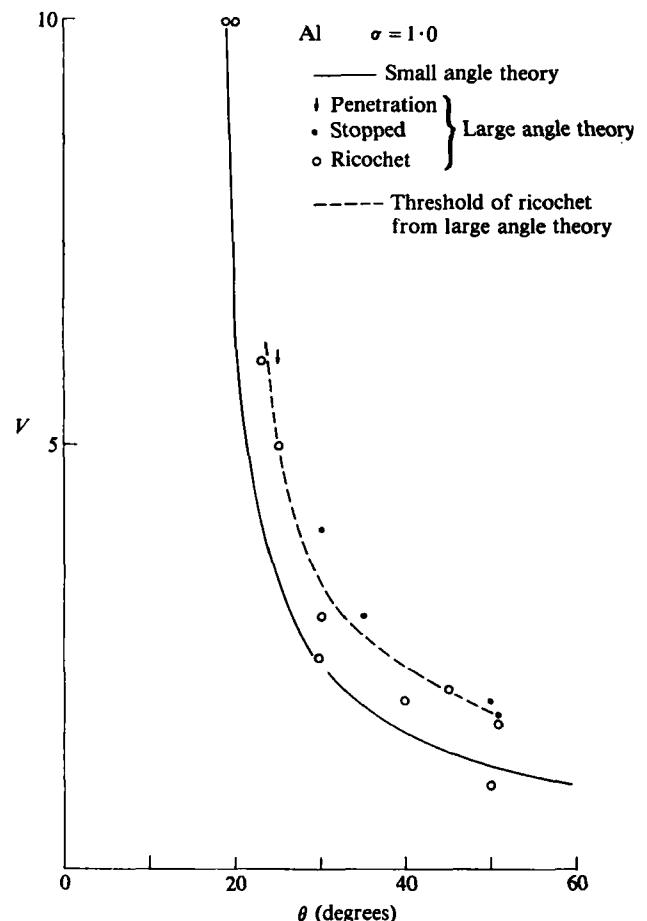

Fig. 3. Calculated dependence of critical impact angle on impinging velocity for aluminium sphere; ricochet off sand

(1) For $\phi_0 = \pi$, $v > 0$, $\theta > 0$. This implies that when fully submerged, the projectile can move further along the tangent to the trajectory. This of course is penetration.

(2) For $\theta_0 < \pi$, $v = 0$, $\theta > 0$. This indicates that before the projectile becomes fully wetted, it has stopped. This is also a form of penetration as before.

(3) For $\phi_0 \leqslant \pi$, $v \neq 0$, $\theta = 0$. In small angle impact theory, this situation was referred to as ricochet and if $\phi_0 = \pi$, as critical ricochet. In the present case, the projectile may ricochet off the medium or not. Physically, although the projectile drifts upwards it would stop somewhere inside the material due to friction, gravity, and material resistance, etc., if its velocity was very low. In performing the present calculations a few cases of the projectile ending up so, were obtained. In some cases however the projectile drifted upward and then moved off the surface of material. This latter case was positively identified as ricochet.
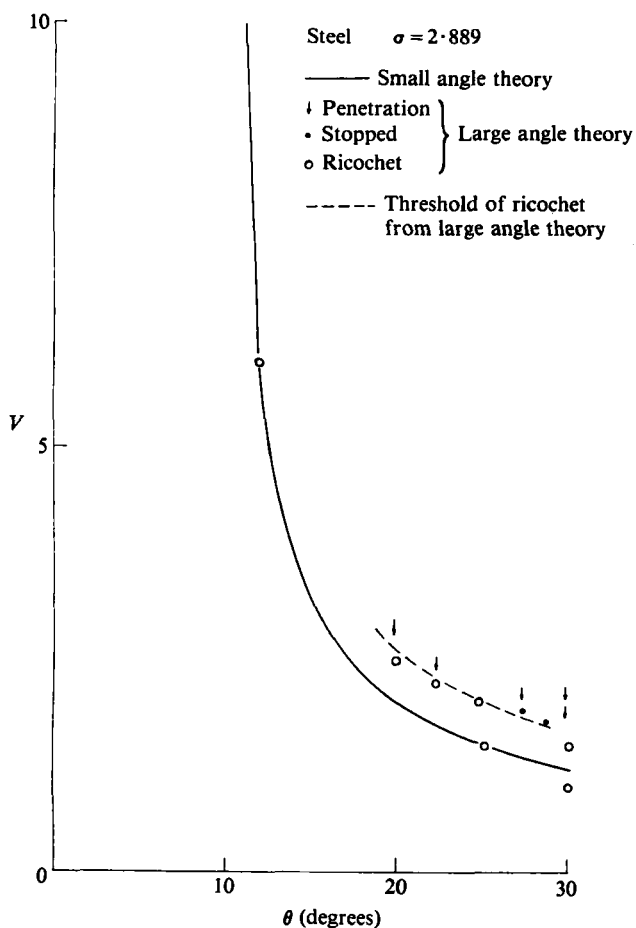

Fig. 4. Calculated dependence of critical impact angle on impinging velocity for steel sphere; ricochet off sand

With the aid of these categories, it is possible to arrive at a critical impact angle versus projectile velocity curve, such as those shown in Figs 3 and 4 for aluminium and steel spheres, respectively. For comparison, small angle theory results also are shown in the corresponding figures. It can be seen that the large angle theory curve lies above that of the small angle theory. As the projectile velocity increases, the critical impact angle decreases and the results for both theories converge.

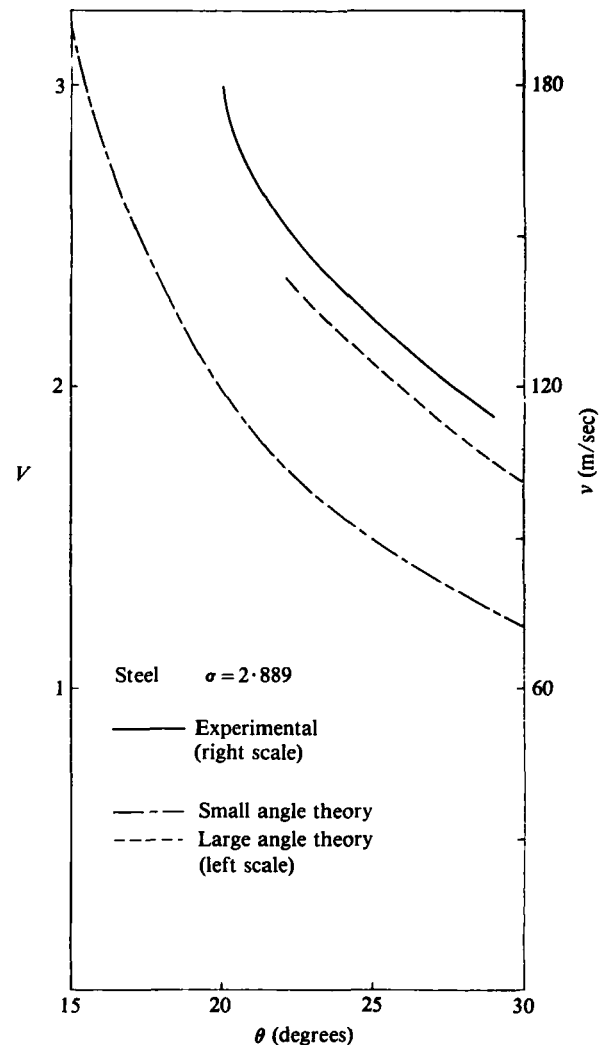In Fig. 5 experimental results and the two sets of

Fig. 5. Comparison of calculated and experimental dependence of critical impact angle on impinging velocity for steel sphere; ricochet off sand

theoretical results for steel projectiles are shown to different scales. It is clear that all of them have nearly the same tendency. If the scale of the dimensionless velocity (the left scale) is changed then the theoretical results can be made to fit with the experimental ones.

Another interesting aspect pertains to the experimentally obtained cut-off angle of 29 degrees for a steel sphere when the dimensionless velocity is approximately 1·75 and 1·25, respectively, for large and small angle theories. Supposing that there is a constant projectile velocity for the ricochet cut-off angle for different pro-

Table 1   Cut-off angle

	Steel (degrees)	Aluminium (degrees)	Lead (degrees)	v (m/sec)	V
Experimental	29	26	51	350	—
Large angle theory	(29)†	23	52	—	1·75
Small angle theory	(29)	24	49	—	1·25

† This is entered in brackets because this magnitude is used to fit the theoretical results.

jectile materials, then from the curves of critical impact angle versus impact velocity as obtained from the various theories, a prediction of the cut-off angle can be obtained. This is shown in Table 1.
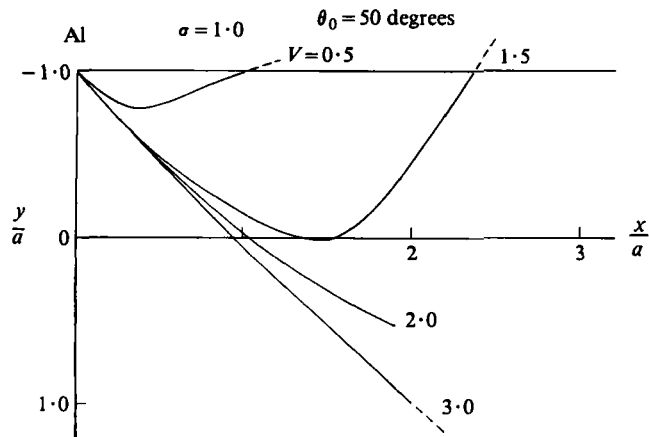

Fig. 6. Trajectories of an aluminium sphere in sand for different impinging velocities at an impact angle of 50 degrees
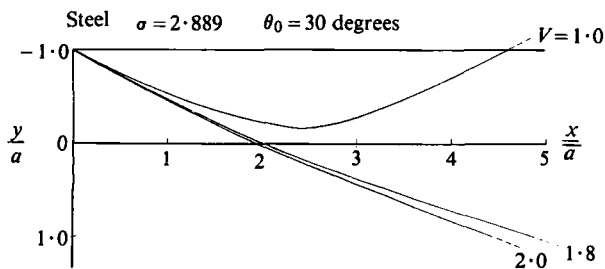

Fig. 7. Trajectories of a steel sphere in sand for different impinging velocities at an impact angle of 30 degrees
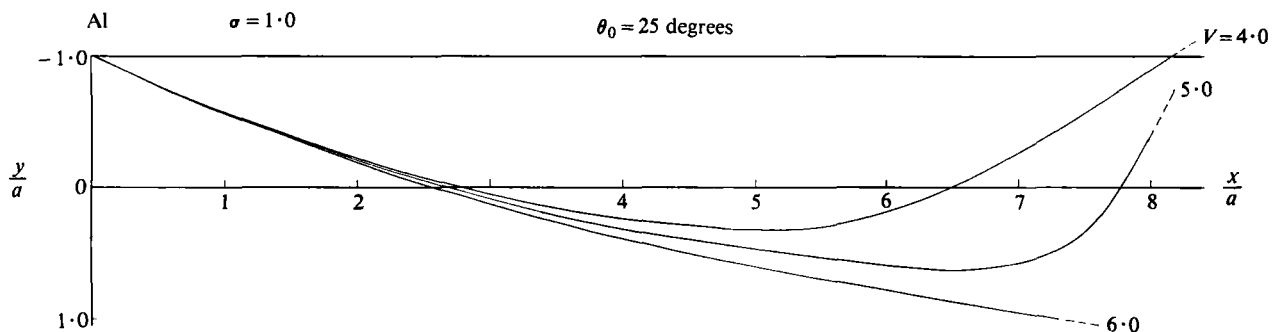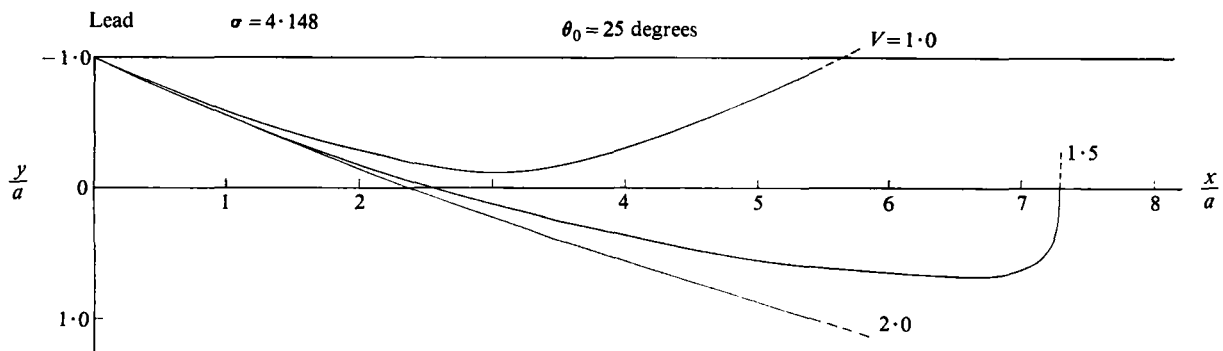
By reference to the observed cut-off velocity of 107 m/sec, the dimensionless velocity 1·75 gives $K \simeq 11 \cdot 6$ MPa and 1·25 gives $K \simeq 22 \cdot 8$ MPa. These values of K seem reasonable for sand.

The reason for the existence of a ricochet cut-off angle is still not clear. However, from the above calculations, it does appear to be related to the inter-relationship between the hydrodynamic pressure and the material resistance. Supposing that the projectile velocity is lower than the value at which the hydrodynamic pressure is roughly equal to the material resistance, then the quasi-steady ideal flow régime might no longer apply so that the lift, which comes from the hydrodynamic pressure, might be severely reduced. The problem may then be converted into that of the penetration of a projectile into a deformable body. Whether this hypothesis is correct or not needs further study.

It is interesting to compare the trajectories for different initial angles of impact and velocity. Pure penetration of a medium implies that the projectile must stop somewhere inside it and an important point then is that with lower impact velocity, the point of trajectory termination rises, particularly in large impact angle cases, i.e., near to the cut-off angle. For some termination points the sphere is found not to have been fully submerged in the medium. This means that before the projectile gains maximum lift, its kinetic energy has been exhausted (see Figs 6, 7, 8 and 9). These calculated trajectories are similar to the types of trajectory identified by Richardson (4), shown in Fig. 10.

Lastly, it is worth mentioning that the exit angles increase dramatically when approaching critical ricochet at large impact angle. This result which has not previously been obtained even by small angle theory, is in agreement with experimental observations (5).
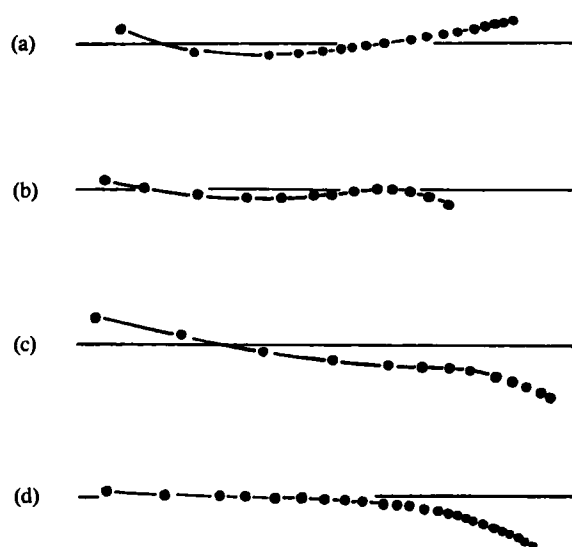

Fig. 8. Trajectories of an aluminium sphere in sand for different impinging velocities at an impact angle of 25 degrees

Fig. 9. Trajectories of a lead sphere in sand for different impinging velocities at an impact angle of 25 degrees

Fig. 10. Four types of trajectory identified by Richardson, from (4)

5 CONCLUSIONS

Taking both weight of the projectile and static pressure in the impacted medium into account the impact velocity dependence of the critical impact angle for ricochet can be accounted for. It also reveals the different tendencies due to this velocity dependence at ricochet off water and sand.

Based on these suppositions a more accurate model is established, with some of the Birkhoff assumptions modified. The velocity of the projectile need no longer be considered constant and the angle of impact could be considered large. In addition, 'flying-off' the surface is adopted as the definition of ricochet, rather than attaining a horizontal velocity at just complete immersion as is used in the Birkhoff approach.

Numerical simulation shows that for small angles of impact the simplified small angle theory is indeed suffi-ciently accurate. But at greater impact angles, a more general model, capable of accommodating large angles of impact with variations in the projectile velocity and the above ricochet condition or definition must be used. This model reveals the termination of the projectile trajec-tory before gaining maximum lift at large impact angles and the phenomenon of dramatic increase in exit angle. Further, by supposing that the ideal fluid régime, (which is responsible for the lift), ceases to be operative below some particular impact velocity and by fitting the theoretical curves to known experimental ones, the rico-chet cut-off angles are 29 degrees, 23 degrees, and 52 degrees for steel, lead, and aluminium spherical projectiles, respectively, the observed values being 29 degrees, 26 degrees, and 51 degrees; the above corre-sponding static resistance of the sand used is implied to have been about 11·6 MPa.

APPENDIX

REFERENCES

(1) JOHNSON, W. and REID, S. R. 'Ricochet of spheres off water', *J. mech. Engng Sci.*, 1975, 17, 71–81.
(2) SOLIMAN, A. S., REID, S. R. and JOHNSON, W. 'The effect of spherical projectile speed in ricochet off water and sand', *Int. J. Mech. Sci.*, 1976, 18, 279–284.
(3) TATE, A. 'Modification of the classical hydrodynamic theory as applied to the penetration of long rods', *J. Mech. Phys. Solids*, 1969, 17, 141.
(4) RICHARDSON, E. G. 'The impact of a solid on a liquid surface', *Proc. Phys. Soc.*, 1948, 61, 352–367.
(5) JOHNSON, W. and DANESHI, G. H. 'Results for the single ricochet of spherical-ended projectiles off sand and clay at up to 400 m/s', in *High velocity deformation of solids* (Edited by Kozo Kawata and Jumpei Shiori), 1979 (Springer Verlag, Berlin) pp. 317–343.